NACA TN 2022 -

NATIONAL ADVISORY COMMITTEE FOR AERONAUTICS

TECHNICAL NOTE 2022

PROPELLER FLIGHT INVESTIGATION TO DETERMINE

THE EFFECTS OF BLADE LOADING

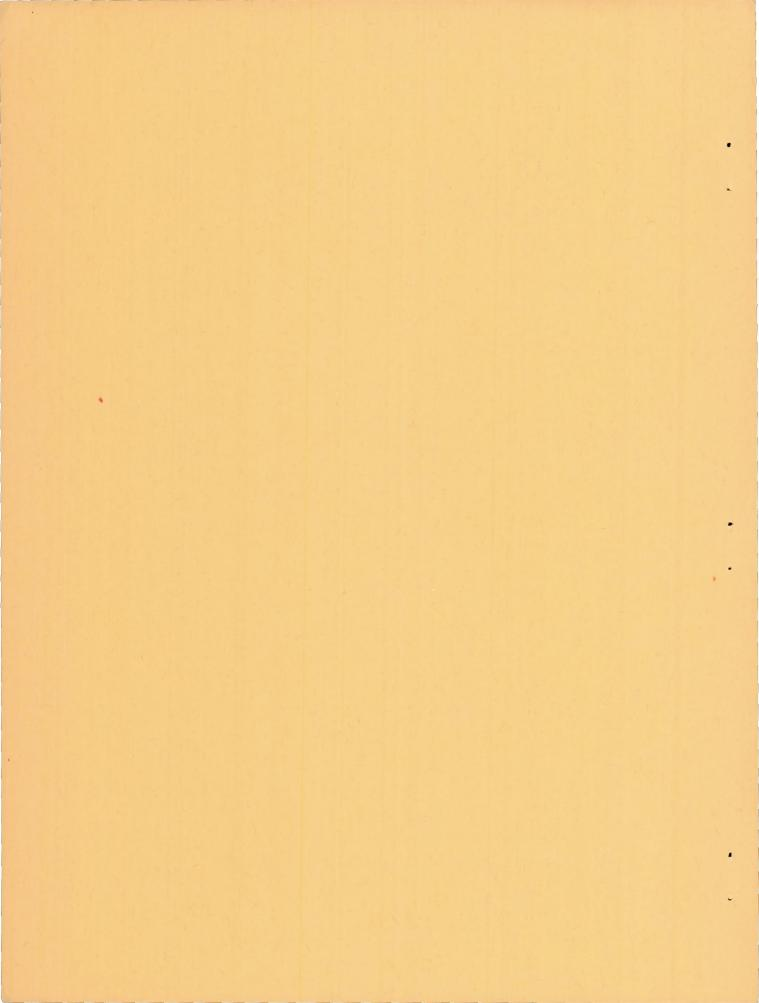
By Jerome B. Hammack and A. W. Vogeley

Langley Aeronautical Laboratory Langley Air Force Base, Va.



Washington January 1950





NATIONAL ADVISORY COMMITTEE FOR AERONAUTICS

TECHNICAL NOTE 2022

PROPELLER FLIGHT INVESTIGATION TO DETERMINE

THE EFFECTS OF BLADE LOADING

By Jerome B. Hammack and A. W. Vogeley

SUMMARY

A flight investigation has been made of a three-blade propeller in climb and at high speed to determine the effects of blade power loading. Increasing the blade power coefficient from 0.06 to 0.09 was found to increase the efficiency approximately 8 percent at an airplane Mach number of 0.7 and a propeller-tip Mach number of 1.13. Further increasing the blade power coefficient from 0.12 to 0.16 increased propeller efficiency 4 percent at an airplane Mach number of 0.7 and a propeller-tip Mach number of 1.07. These increases were shown to be caused primarily by a reduction in profile drag losses.

In climb, an increase in power loading was shown to reduce efficiency, as a consequence of increased induced drag losses. Profile losses, except where blade stall was encountered, were of secondary importance.

INTRODUCTION

The effects of blade power loading on the characteristics of a three-blade propeller have been investigated by climb and high-speed flight tests. Climbs were made at an indicated airspeed of 165 miles per hour. High-speed tests were made up to an airplane Mach number of 0.7 and to a propeller-tip Mach number of about 1.1. Blade power coefficients from 0.06 to 0.16 were investigated.

The present paper includes data previously published in reference las well as data obtained in the present investigation. The two investigations were made with two radial-engine fighter airplanes differing mainly in engine power ratings and slightly in propeller gear ratio. The two series of data have been correlated, and a brief discussion is given on the effects of blade power loading on propeller operation.

SYMBOLS

ъ	blade-section width, feet
В	number of blades
CZ	section lift coefficient
cld	design section lift coefficient
$C_{\mathbf{P}}$	propeller power coefficient $\left(\frac{P}{\rho n^3 D^5}\right)$
$\mathtt{c}_{\mathtt{T}}$	propeller thrust coefficient $\left(\frac{T}{\rho n^2 D^4}\right)$
$\frac{dC_{\mathrm{T}}}{d(x_{\mathrm{S}})^{2}}$	element thrust coefficient
D	propeller diameter, feet
h	blade-section maximum thickness, feet
J	advance ratio $\left(\frac{V}{nD}\right)$
М	airplane Mach number
Mt	helical Mach number
n	propeller rotational speed, rps
P	engine power supplied to propeller, foot-pounds per second
R	propeller tip radius, feet
r	radius to blade element, feet
r _s	radial distance from thrust axis to survey point, feet
Т	propeller thrust, pounds
V	forward speed, miles per hour
$x = \frac{r}{R}$	
$x_{B} = \frac{r_{B}}{R}$	

PROPELLER AND TEST EQUIPMENT

General specifications of the propeller and engine used in the present investigation and those of reference 1 are as follows:

Specifications	Airplane of present investigation	Airplane of reference 1
Number of blades	3 Hamilton Standard No. 6507A-2	3 Hamilton Standard No. 6507A-2
Approximate design lift coefficient	0.4 NACA 16 series 12.92	0.4 NACA 16 series 12.83
ratio	0.45:1 Pratt and Whitney R-2800-73	0.50:1 Pratt and Whitney R-2800-59
Normal power rating of engine: Engine speed, rpm	42.5	2550 42 1625
Military power rating of engine Engine speed, rpm Manifold pressure,	2800	2700 52
inches of mercury Brake horsepower	63.00	2000
War-emergency power rating of engine: Engine speed, rpm	. 72	
Brake horsepower	2800	

Blade-form curves of the propeller are presented in figure 1. A photograph of a typical installation and airplane is shown in figure 2.

Propeller thrust was measured by the slipstream-survey method and engine power by a torque meter supplied by the engine manufacturer. The test equipment, test procedures, and method of reduction of data were identical with those described in reference 2.

RESULTS

The behavior of the propeller in a normal power climb is shown in figure 3. In this figure, the variations of advance ratio, thrust and power coefficients, efficiency, and propeller-tip and airplane Mach numbers with density altitude are given. Typical thrust-distribution curves for the normal power climb are presented in figure 4. Similarly, the characteristics of the propeller in a military power climb are given in figures 5 and 6 and in a war-emergency power climb, in figures 7 and 8.

The characteristics of the propeller at high speed are presented in figure 9 as the variation of efficiency with airplane Mach number for several values of blade power loading. In figure 10 is given the variation of propeller efficiency with blade power loading at an airplane Mach number of 0.7. In figure 10 data for two values of tip Mach number are given because a slight difference in propeller gear ratio exists between the two test airplanes.

In figure 11 are presented thrust-distribution curves for the relatively low blade power coefficient of 0.08 over the airplane Mach number range from 0.430 to 0.713. Thrust distributions for the highest blade loading tested, 0.16, and over essentially the same Mach number range are given in figure 12.

ANALYSIS AND DISCUSSION

As blade power loading was increased, the Mach number at which maximum propeller efficiency was attained was increased as can be seen in figure 9. As a consequence, at the maximum airplane Mach number of 0.7, an increase in blade power loading resulted in an increase in propeller efficiency. At an airplane Mach number of 0.7 and a tip Mach number of 1.13 (for the airplane of reference 1), an increase in the blade power coefficient from 0.06 to 0.09 can be seen from figure 10(a) to result in an 8-percent gain in propeller efficiency.

At the same airplane Mach number of 0.7, but at the lower tip Mach number of 1.07 (due to the lower propeller rotational speed of the airplane of the present investigation), an increase in blade power coefficient from 0.12 to 0.16 resulted in an increase in propeller efficiency of 4 percent. (See fig. 10(b).)

From an analysis of the profile and induced losses, the main effect of an increase in power loading was found to be a reduction in profile-drag losses in regions of operation where compressibility losses occur. Determination of the reason for the increase in efficiency with increase in power loading requires knowledge of the operating lift coefficients. Behavior of the section lift coefficient for high-speed flight at a sample radial station of 0.7R is shown in figure 13. The lift-coefficient curves were obtained from a simple blade-element theory with the use of the measured values of section thrust loading and reasonable assumed values of section lift-drag ratio. From this figure, the increase in section lift coefficients with power loading may be seen.

It is interesting to note that for the test propeller the highest measured efficiency at an airplane Mach number of 0.7 (fig. 10) was obtained when the design station of 0.7R was operating at a lift coefficient of 0.7 (fig. 13) rather than at its design lift coefficient of 0.4 (fig. 1). Furthermore, because of insufficient engine power the blade loading for maximum efficiency was not reached; this fact indicates that better section efficiencies would be obtained at still higher blade loadings and section lift coefficients. This result is deemed reasonable in view of reference 3 which shows that at high subcritical Mach numbers, maximum section lift-drag ratio is obtained with NACA 16-series airfoils at a lift coefficient which is always higher than the design lift coefficient.

Other factors affecting the variation of high-speed efficiency with power loading are the axial and rotational induced losses. At high forward speeds and at advance ratios in the range of these tests, the induced losses are, from calculations, generally small with respect to the profile losses. Although the induced losses will increase with power loading, to a small extent the increase is alleviated by the improvement in thrust distribution of this propeller as the blade power coefficient is increased. The induced losses are a minimum when a Betz distribution, which may be approximated by an elliptical distribution of thrust with the square of the propeller radius, is obtained. Figure 14 presents the variation in thrust distribution with blade power loading at an airplane Mach number of 0.7. In the figure, the thrust-distribution coefficients have been multiplied by J/Cp to compensate for the variation in power coefficient and advance ratio between the tests. It is seen that the thrust distribution more nearly approaches an elliptical distribution as the power loading is increased so that the normal increase in induced losses with power

is somewhat compensated by the more favorable distribution. Even so, the trend is for the induced losses to increase with power loading, and a net gain in efficiency must therefore be the result of a reduction in profile losses.

In climbs, an analysis shows that the variation of efficiency with power loading is caused primarily by the change in induced losses and, in contrast to the high-speed case, only secondarily by the change in profile losses. This fact is illustrated in figures 3 and 5 in which little change in efficiency occurs throughout the climbing range. These climbs cover a wide range of blade power coefficients, but at the same time the advance ratios are varying in such a manner that the effects of advance ratio on the induced losses compensate for the effects of power loading. In the climb of figure 7, however, not only is the general level of efficiency lower than in the previous climb, but the efficiency decreases with altitude. In this case, because of the rapidly increasing power coefficient, the induced losses due to power loading are not compensated by the effect of increasing advance ratio.

Profile losses are in evidence in figure 7 and can be seen graphically in figure 8(f). Profile losses in climbs are only important when power loading is increased to such an extent as to cause blade stall; this increase resulted in such a condition as shown in the previously mentioned figure (fig. 8(f)) and, again, in figure 15. In the present investigation noticeable blade stall losses were encountered in only one power condition - that of war-emergency power climb.

CONCLUDING REMARKS

A flight investigation has been made of a three-blade propeller in climb and at high speed to determine the effects of blade power loading. Increasing the blade power coefficient from 0.06 to 0.09 increased propeller efficiency approximately 8 percent at an airplane Mach number of 0.7 and a propeller-tip Mach number of 1.13. Further increasing the blade power coefficient from 0.12 to 0.16 increased propeller efficiency 4 percent at an airplane Mach number of 0.7 and a propeller-tip Mach number of 1.07. These increases were shown to be caused primarily by a reduction in profile drag losses.

In climb, an increase in power loading over the range of blade power coefficients investigated was shown to reduce efficiency, as a consequence of increased induced drag losses. Profile losses, except where blade stall was encountered, were of secondary importance.

Langley Aeronautical Laboratory
National Advisory Committee for Aeronautics
Langley Air Force Base, Va., December 2, 1949

REFERENCES

- 1. Gardner, J. J.: Effect of Blade Loading on the Climb and High-Speed Performance of a Three-Blade Hamilton Standard No. 6507A-2 Propeller on a Republic P-47D Airplane. NACA MR L5G09a, 1945.
- 2. Vogeley, A. W.: Climb and High-Speed Tests of a Curtiss No. 714-1C2-12 Four-Blade Propeller on the Republic P-47C Airplane. NACA ACR L4L07, 1944.
- 3. Lindsey, W. F., Stevenson, D. B., and Daley, Bernard N.: Aerodynamic Characteristics of 24 NACA 16-Series Airfoils at Mach Numbers between 0.3 and 0.8. NACA TN 1546, 1948.

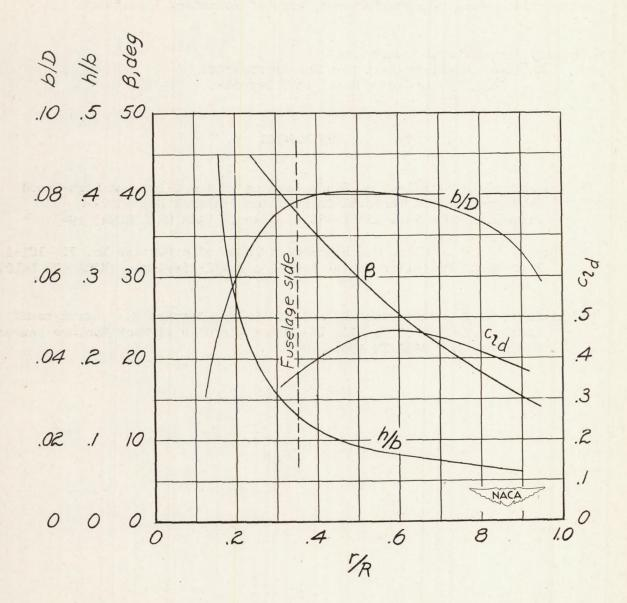


Figure 1.- Blade-form curves for a three-blade propeller.

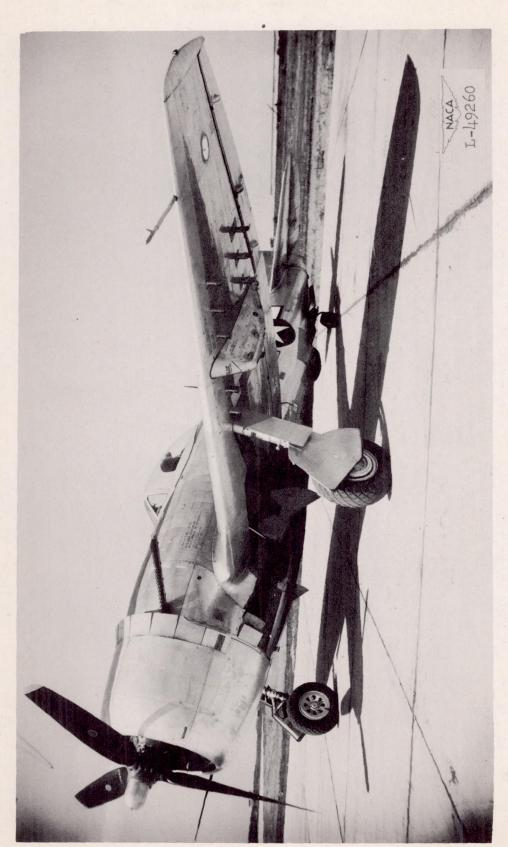
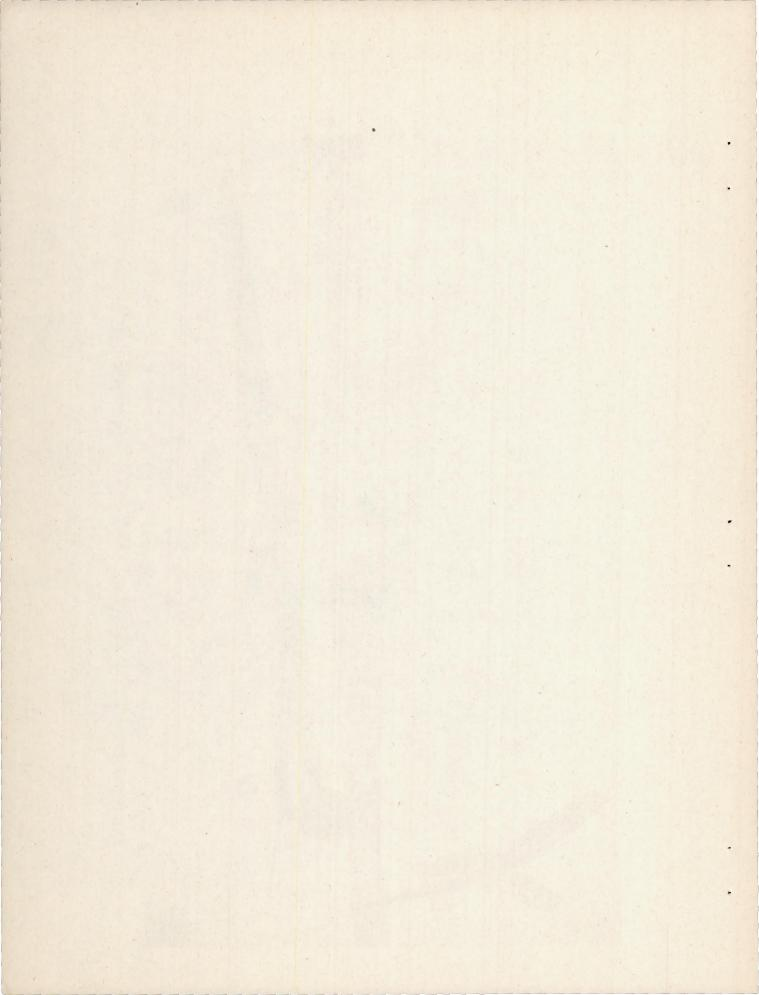


Figure 2. - Typical installation of propeller and test equipment on airplane.



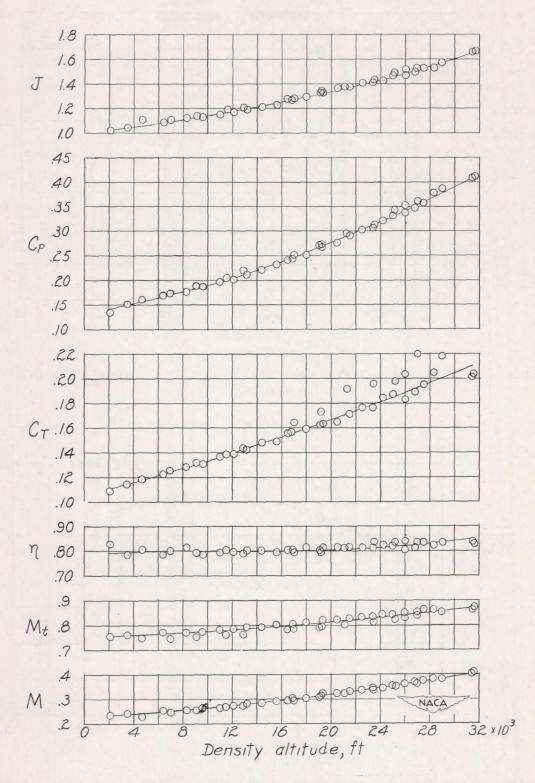
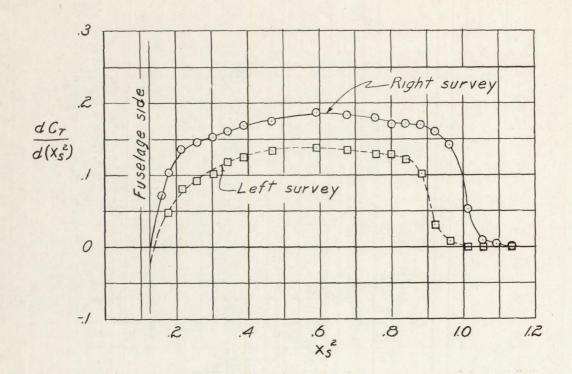
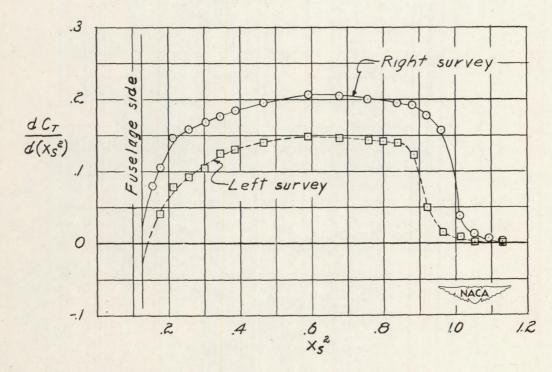


Figure 3.- Normal power climb at an indicated airspeed of 165 miles per hour with a three-blade propeller on airplane of present investigation.

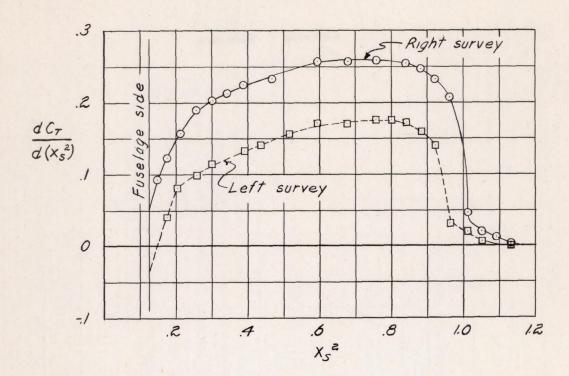


(a) J = 1.046; Cp = 0.153; CT = 0.115; $\eta = 78.4$ percent; M = 0.240; $M_t = 0.761$.

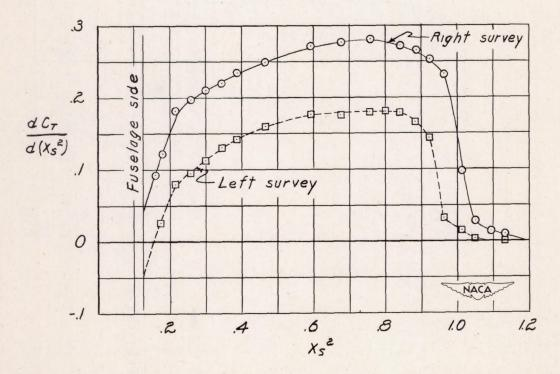


(b) J = 1.125; $C_P = 0.177$; $C_T = 0.129$; $\eta = 81.9$ percent; M = 0.260; $M_t = 0.770$.

Figure 4.- Thrust-distribution curves for normal power climb. Three-blade propeller on airplane of present investigation.

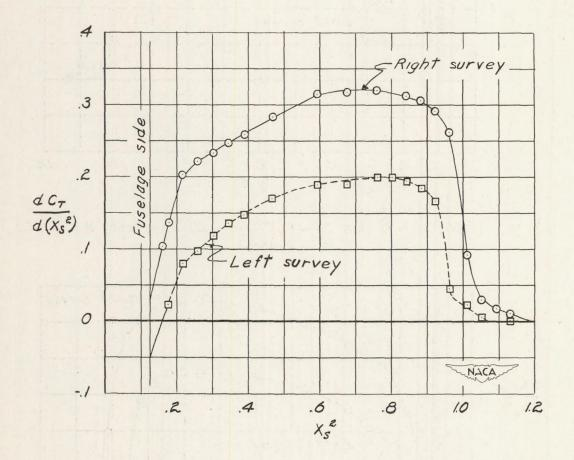


(c) J = 1.264; $C_P = 0.245$; $C_T = 0.157$; $\eta = 80.8$ percent; M = 0.301; $M_t = 0.807$.



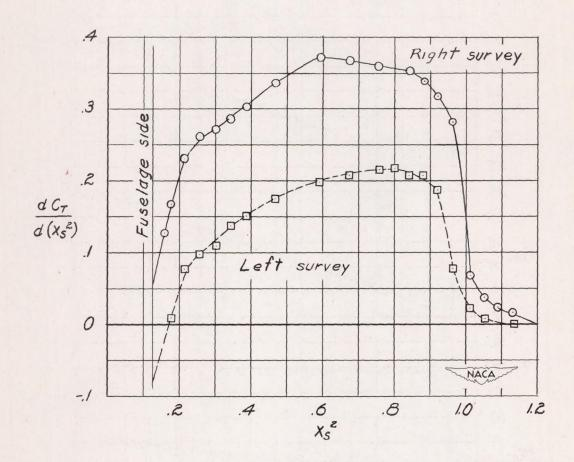
(d) J = 1.360; $C_P = 0.276$; $C_T = 0.165$; $\eta = 81.5$ percent; M = 0.327; $M_t = 0.824$.

Figure 4.- Continued.



(e) J = 1.426; $C_P = 0.321$; $C_T = 0.185$; $\eta = 82.2$ percent; M = 0.349; $M_t = 0.845$.

Figure 4.- Continued.



(f) J = 1.532; $C_P = 0.379$; $C_T = 0.205$; $\eta = 82.6$ percent; M = 0.380; $M_t = 0.868$.

Figure 4.- Concluded.

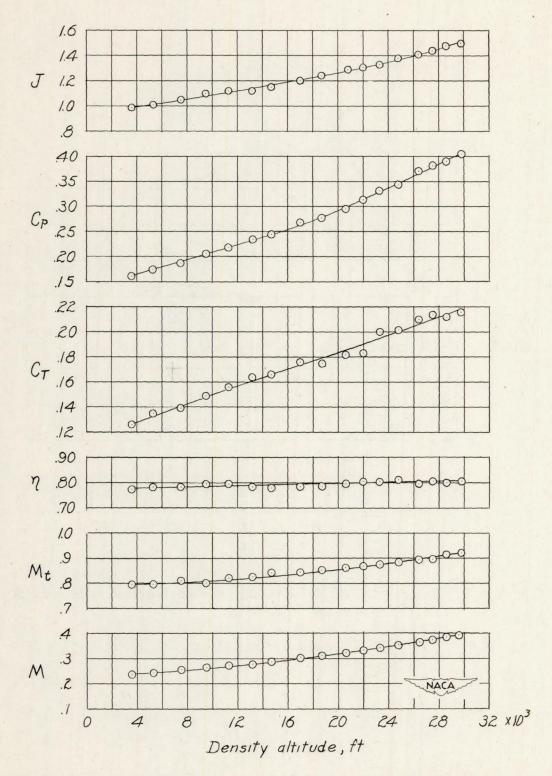
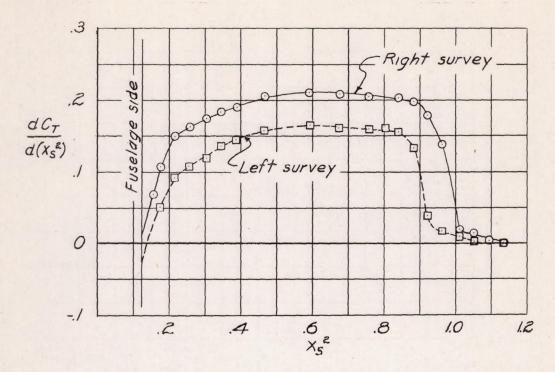
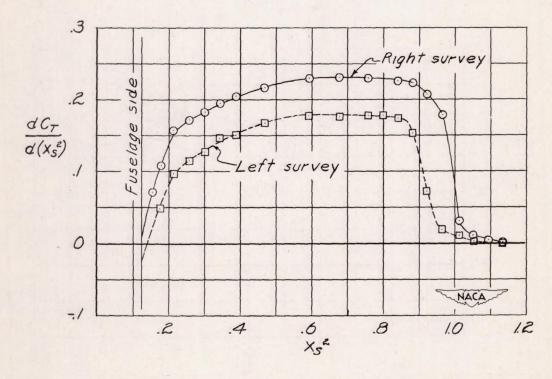


Figure 5.- Military power climb at an indicated airspeed of 165 miles per hour with a three-blade propeller on airplane of present investigation.

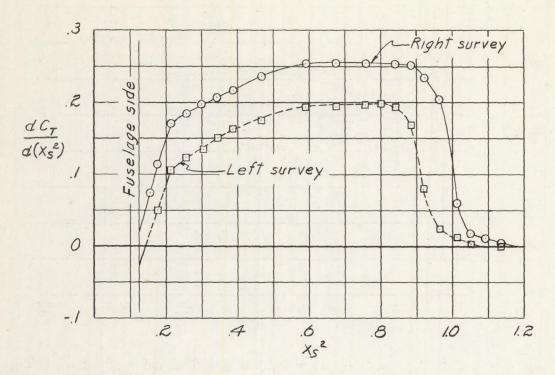


(a) J = 1.007; Cp = 0.174; $C_T = 0.135$; $\eta = 78.2$ percent; M = 0.244; $M_t = 0.797$.

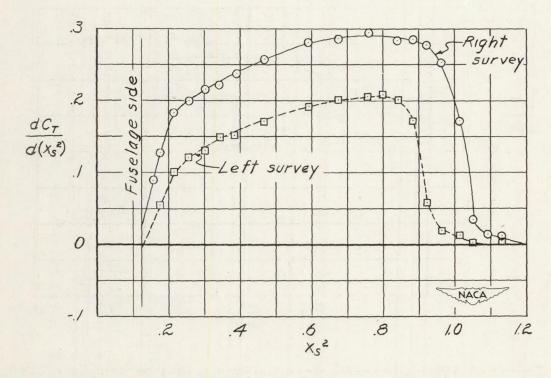


(b) J = 1.099; $C_P = 0.206$; $C_T = 0.149$; $\eta = 79.6$ percent; M = 0.265; $M_t = 0.801$.

Figure 6.- Thrust-distribution curves for military power climb. Three-blade propeller on airplane of present investigation.

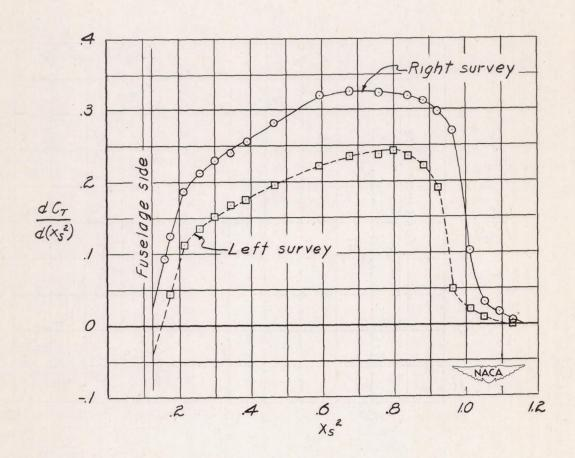


(c) J = 1.123; $C_P = 0.235$; $C_T = 0.164$; $\eta = 78.3$ percent; M = 0.279; $M_t = 0.829$.



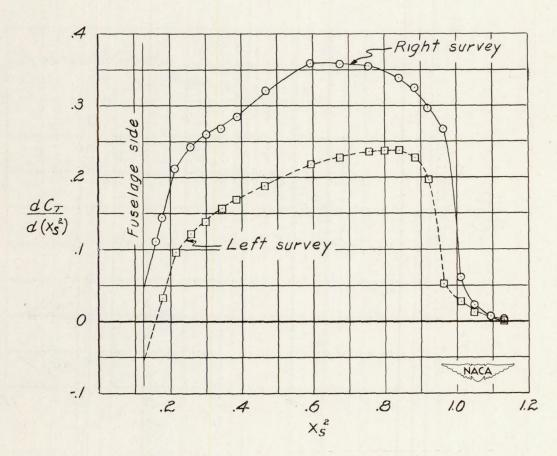
(d) J = 1.119; $C_P = 0.268$; $C_T = 0.176$; $\eta = 78.7$ percent; M = 0.302; $M_t = 0.845$.

Figure 6.- Continued.



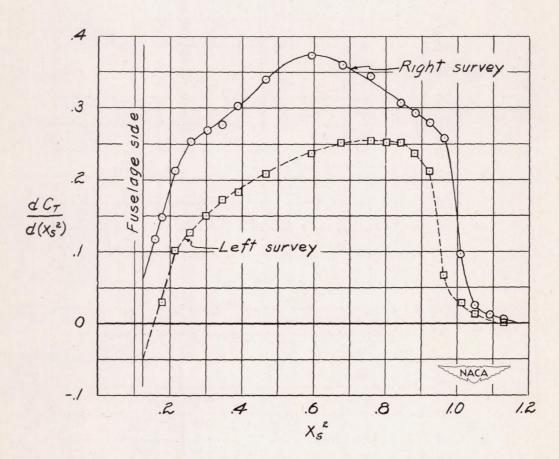
(e) J = 1.331; $C_P = 0.331$; $C_T = 0.200$; $\eta = 80.6$ percent; M = 0.343; $M_t = 0.878$.

Figure 6. - Continued.



(f) J = 1.411; $C_P = 0.371$; $C_T = 0.210$; $\eta = 79.8$ percent; M = 0.367; $M_t = 0.895$.

Figure 6.- Continued.



(g) J = 1.503; $C_P = 0.404$; $C_T = 0.216$; $\eta = 80.3$ percent; M = 0.398; $M_t = 0.921$.

Figure 6.- Concluded.

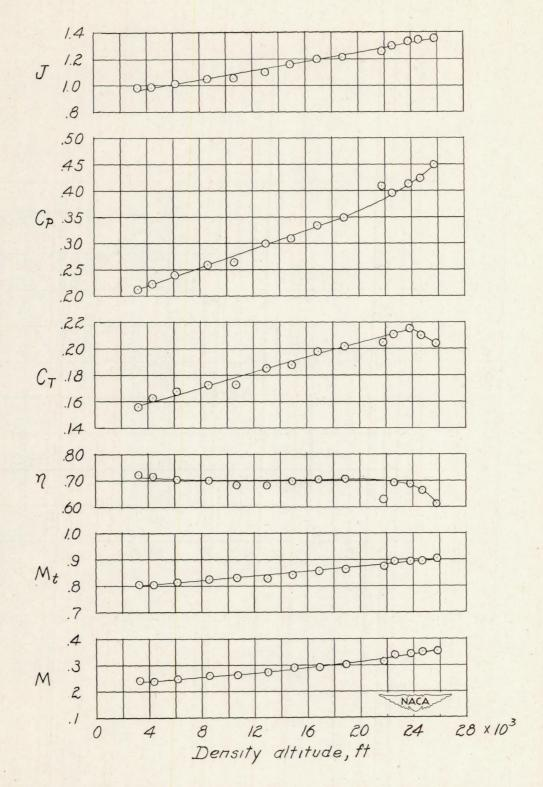
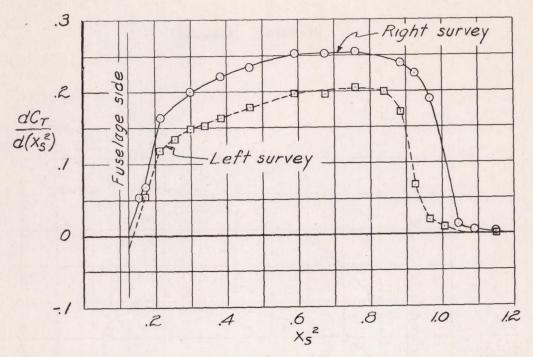
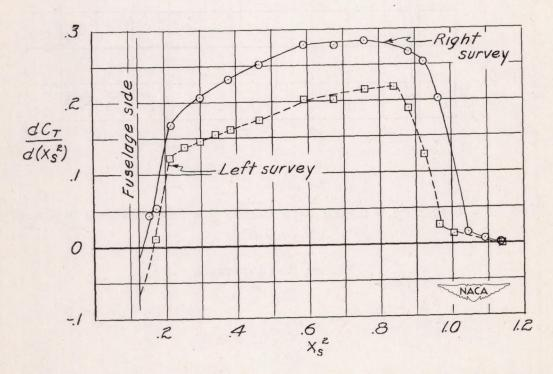


Figure 7.- War-emergency power climb at an indicated airspeed of 165 miles per hour with a three-blade propeller on airplane of present investigation.



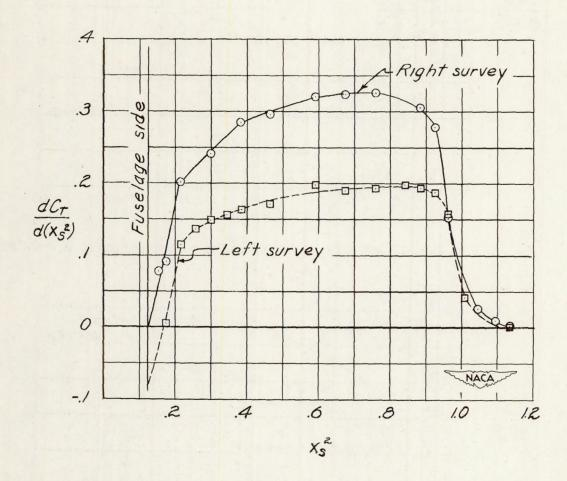
(a) J = 0.985; $C_P = 0.223$; $C_T = 0.163$; $\eta = 71.9$ percent; M = 0.240; $M_t = 0.803$.



(b) J = 1.055; $C_P = 0.259$; $C_T = 0.173$; $\eta = 70.4$ percent; M = 0.262; $M_t = 0.824$.

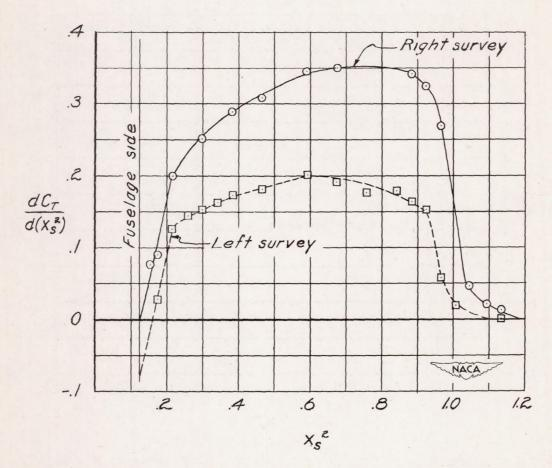
Figure 8.- Thrust-distribution curves for war-emergency power climb.

Three-blade propeller on airplane of present investigation.



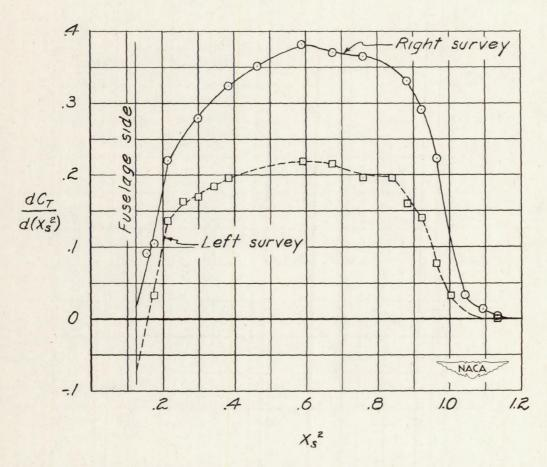
(c) J = 1.102; Cp = 0.300; CT = 0.186; η = 68.4 percent; M = 0.275; $M_{\rm t}$ = 0.831.

Figure 8.- Continued.



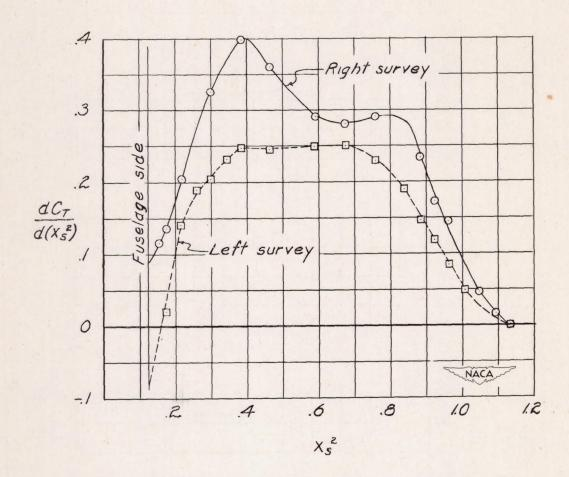
(d) J = 1.198; $C_P = 0.335$; $C_T = 0.198$; $\eta = 70.9$ percent; M = 0.306; $M_t = 0.858$.

Figure 8.- Continued.



(e) J = 1.302; $C_P = 0.395$; $C_T = 0.211$; $\eta = 69.5$ percent; M = 0.341; $M_t = 0.894$.

Figure 8. - Continued.



(f) J = 1.351; $C_P = 0.450$; $C_T = 0.204$; $\eta = 61.2$ percent; M = 0.357; $M_t = 0.903$.

Figure 8. - Concluded.

28

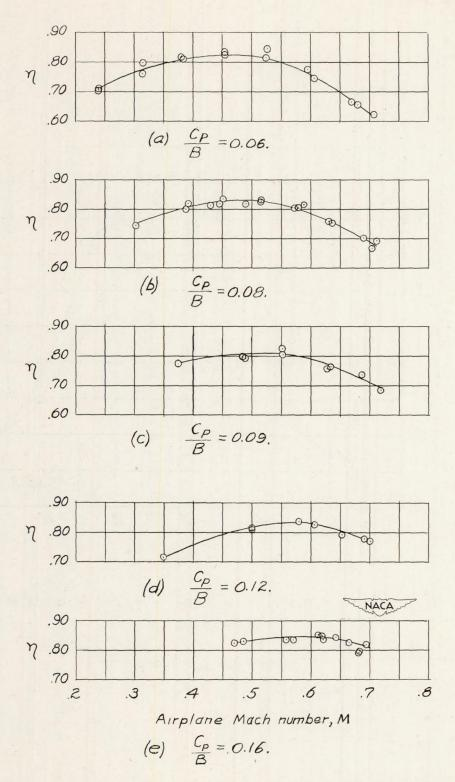


Figure 9.- Behavior of propeller efficiency with airplane Mach number at a series of blade loadings. Three-blade propeller on airplanes of present investigation and reference 1.

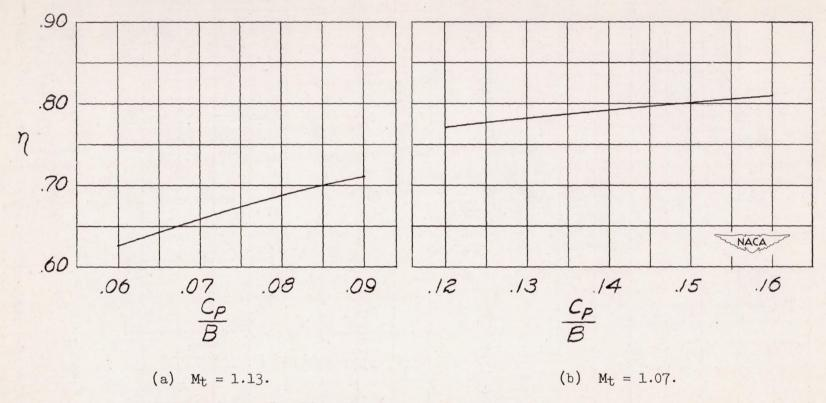
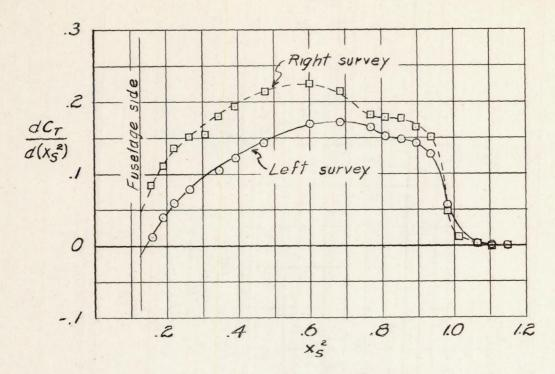
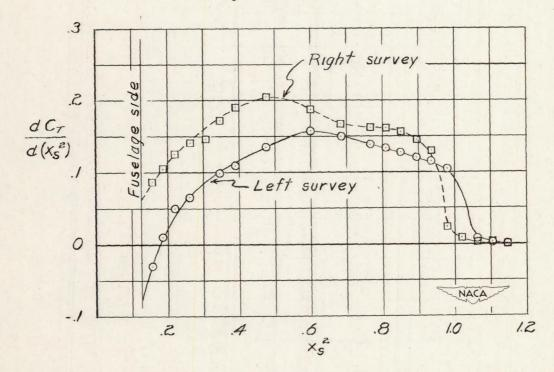


Figure 10.- Effect of blade power coefficient on propeller efficiency at an airplane Mach number of 0.7.

Three-blade propeller on airplanes of present investigation and reference 1.

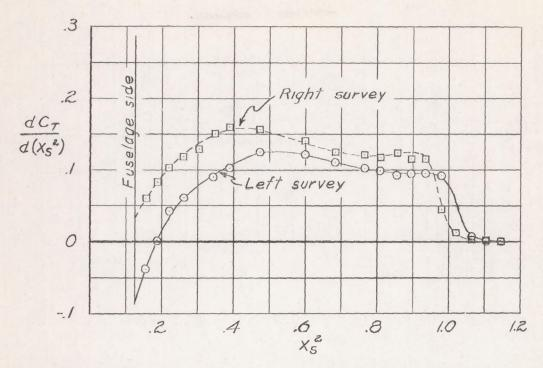


(a) J = 1.488; $C_P = 0.244$; $C_T = 0.1333$; $\eta = 81.3$ percent; M = 0.430; $M_{+} = 1.003$.

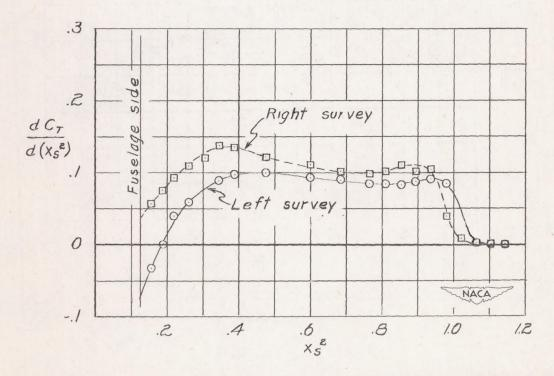


(b) J = 1.694; $C_P = 0.246$; $C_T = 0.1188$; $\eta = 81.9$ percent; M = 0.490; $M_t = 1.032$.

Figure 11.- Thrust-distribution curves made at a blade power coefficient of 0.08 over airplane Mach number range. Three-blade propeller on airplane of reference 1.

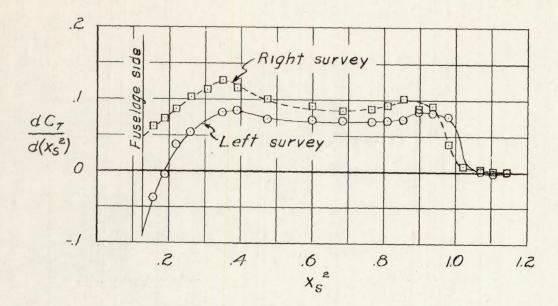


(c) J = 1.990; $C_P = 0.237$; $C_T = 0.0955$; $\eta = 80.1$ percent; M = 0.573; $M_t = 1.071$.

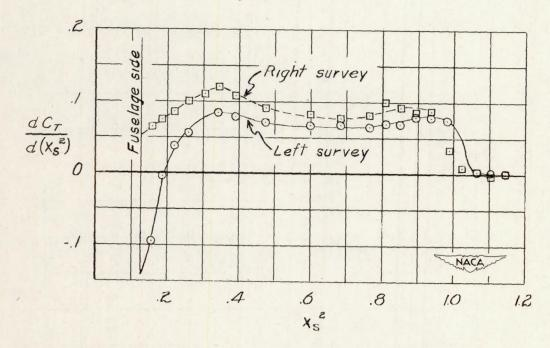


(d) J = 2.225; $C_P = 0.238$; $C_T = 0.0805$; $\eta = 75.3$ percent; M = 0.637; $M_t = 1.103$.

Figure 11. - Continued.



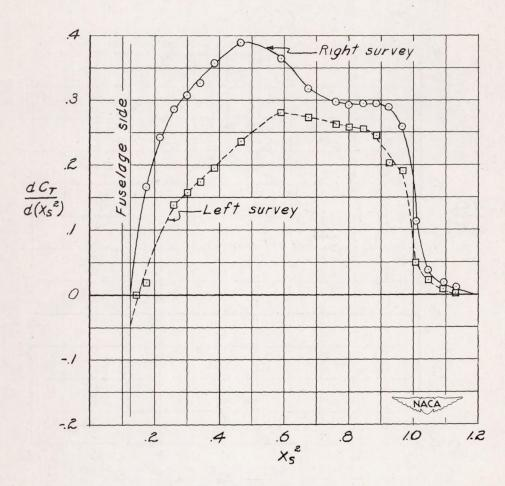
(e) J = 2.403; Cp = 0.233; $C_T = 0.0680$; $\eta = 70.1$ percent; M = 0.690; $M_t = 1.136$.



(f) J = 2.484; $C_P = 0.233$; $C_T = 0.0650$; $\eta = 69.3$ percent; M = 0.713; $M_t = 1.149$.

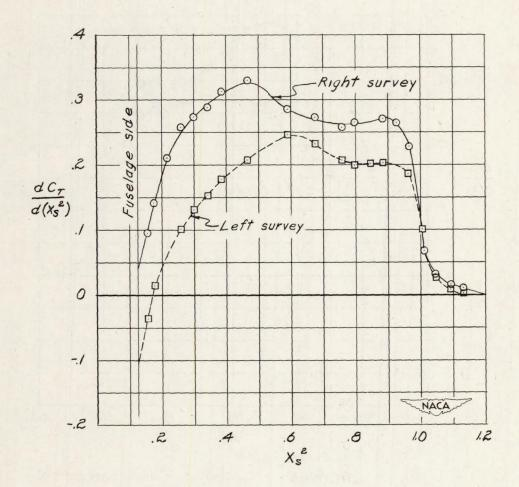
Figure 11. - Concluded.

NACA TN 2022 33



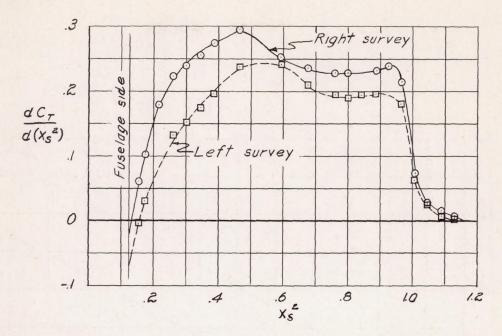
(a) J = 1.728; $C_P = 0.469$; $C_T = 0.2238$; $\eta = 82.4$ percent; M = 0.471; $M_t = 0.976$.

Figure 12.- Thrust-distribution curves made at a blade power coefficient of 0.16 over airplane Mach number range. Three-blade propeller on airplane of present investigation.

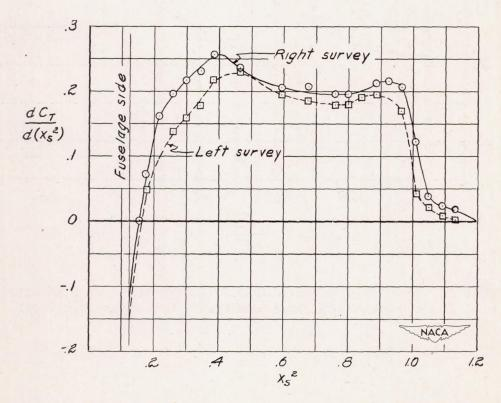


(b) J = 2.054; $C_P = 0.404$; $C_T = 0.1890$; $\eta = 83.7$ percent; M = 0.558; $M_t = 1.020$.

Figure 12. - Continued.



(c) J = 2.304; $C_P = 0.490$; $C_T = 0.177$; $\eta = 83.4$ percent; M = 0.622; $M_t = 1.052$.



(d) J = 2.574; $C_P = 0.477$; $C_T = 0.152$; $\eta = 82.0$ percent; M = 0.694; $M_t = 1.095$.

Figure 12. - Concluded.

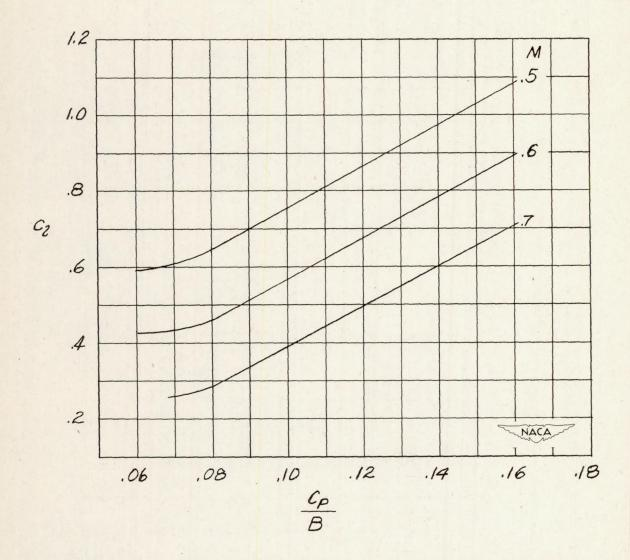


Figure 13.- Variation of section lift coefficients at 0.7R with power loading at several Mach numbers. Three-blade propeller.

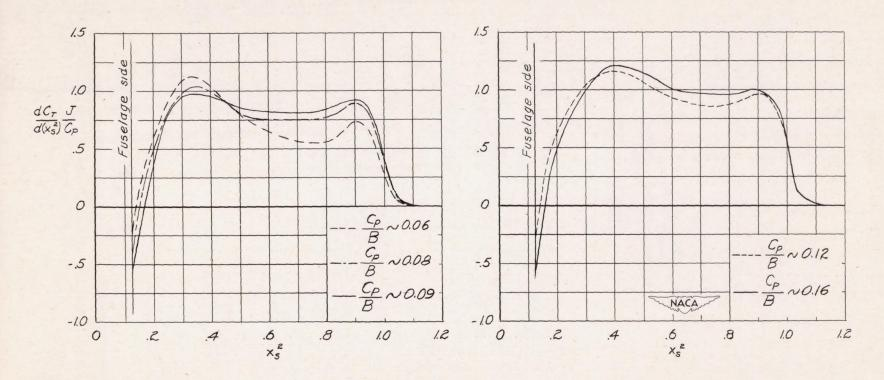


Figure 14.- Thrust-distribution curves for the range of blade loadings tested. Advance ratio, approximately 2.5; airplane Mach number, approximately 0.7.

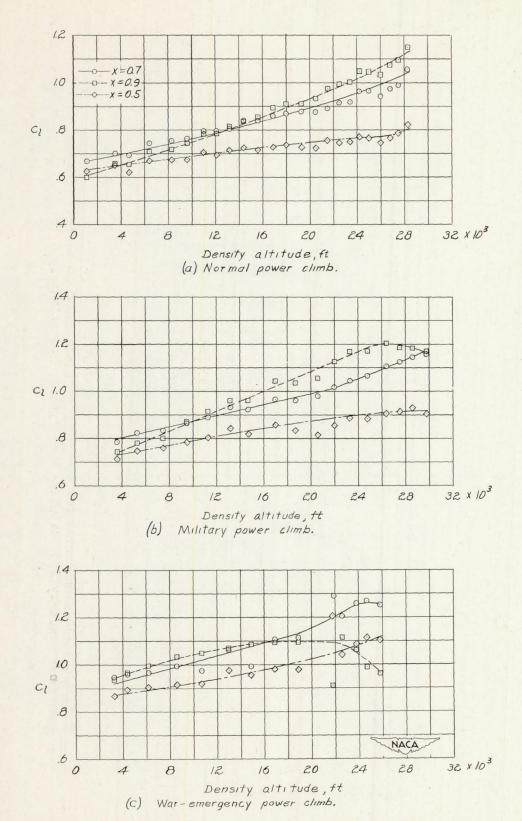


Figure 15.- Variation of section lift coefficients with altitude for a series of climbs. Three-blade propeller on airplane of present investigation.

NACA-Langley - 1-26-50 - 800